Conformation of Micellar Phospholipid Bound to the Active Site of Phospholipase A_2[†]

Leigh A. Plesniak, Lin Yu, and Edward A. Dennis*

Department of Chemistry and Biochemistry, 0601, University of California, San Diego, 9500 Gilman Drive, La Jolla, California 92093-0601

Received September 29, 1994; Revised Manuscript Received January 23, 1995[⊗]

ABSTRACT: Transferred NOE techniques have been used to determine the structure of phospholipid analogues bound to the active site of cobra venom phospholipase A_2 (PLA_2). These experiments were carried out on PLA_2 with a substrate analogue which serves as an inhibitor, 1-(hexylthio)-2-(nonanoylamino)-1,2-dideoxy-*sn*-glycero-3-phosphocholine (PC9). Because this inhibitor binds tightly to the enzyme and forms micelles at millimolar concentrations, experiments could be carried out to determine the conformation of the inhibitor when bound to the enzyme at the lipid−water interface. NOEs of the micellar lipid develop inefficiently in the absence of enzyme. NOESY experiments in the presence of PLA_2 were used to determine the inhibitor structure and conformation when bound to the enzyme. The inhibitor adopts an active site conformation in which the end of the *sn*-2 chain is within 5 Å of the α-methylene protons of the *sn*-1 chain. However, NOE cross-peaks in the experiments indicate that the backbone conformation of the bound lipid is different from that of a shorter chain lipid which forms monomers [Plesniak *et al.* (1993) *Biochemistry 32,* 5009−5016].

Cobra venom phospholipase A_2 (PLA_2)[1] is one of the extracellular phospholipases (Dennis, 1994) that is responsible for the hydrolysis of the *sn*-2 fatty acid of phospholipids at membrane and other lipid−water interfaces (Dennis, 1983). Although this enzyme can catalyze the hydrolysis of monomeric substrates, there is a considerable activation of the enzyme in the presence of aggregated substrates such as micelles and membrane vesicles. This interfacial activation gives rise to an activity that is 10−100-fold greater than the enzyme's activity toward the monomeric form of the substrate (Hazlett *et al.*, 1990).

Amide substrate analogues, which contain an amide group in the place of the *sn*-2 ester group of phospholipids, are potent, reversible inhibitors of PLA_2 (Davidson *et al.*, 1986; Yu *et al.*, 1990; Yu & Dennis, 1992). They bind to the enzyme about 3 orders of magnitude tighter than substrate in a pH-dependent manner (Yu & Dennis, 1991). The structure of an amide analogue at the active site of PLA_2 has been elucidated at the atomic level by X-ray crystallographic studies (Thunnissen *et al.*, 1990). Recently, we have employed NMR approaches to determine the structure of a monomeric amide analogue bound to the active site of PLA_2 in solution (Plesniak *et al.*, 1993). However, all of the structures determined so far are limited to monomeric substrate analogues in the absence of a lipid interface. Other investigators (Dekker *et al.*, 1991; Peters *et al.*, 1992) have observed changes at pH 5 in porcine pancreatic PLA_2 chemical shifts and structure upon association with deuterated DODPC micelles as well as a single-chain alkyl amide inhibitor imbedded in the DODPC micelles. These studies showed intermolecular NOEs between the inhibitor and the PLA_2 but not specific intramolecular NOEs within the inhibitor. We have now synthesized an amide phospholipid that can form micelles by itself with an optimal CMC for transferred NOE studies and used it to determine intramolecular NOEs and the structure and conformation of the inhibitor in micellar form when bound to PLA_2 at physiological pH.

EXPERIMENTAL PROCEDURES

Materials. Cobra venom PLA_2 (*Naja naja naja*) was purified as described elsewhere (Hazlett & Dennis, 1985b; Reynolds & Dennis, 1991) and stored frozen at −20 °C. Inactivation of phospholipase A_2 with *p*-bromophenacyl bromide (BPB) (Roberts *et al.*, 1977) was previously described (Plesniak *et al.*, 1993). All NMR solvents and deuterated dodecylphosphocholine (DODPC) were purchased from Cambridge Isotope Laboratories.

Preparation of Amide Phospholipid Analogues. The synthesis of thioether amide analogues was reported previously (Yu *et al.*, 1990; Plesniak *et al.*, 1993; Bhatia & Hajdu, 1988). We (Yu & Dennis, 1992) have now developed an alternative approach to the synthesis of these thioether amide phosphatidylcholine analogues which allows one to easily change the length of the fatty acid at the *sn*-2 position.

[†] This work was supported by NIH Grant GM 20501. The NMR spectrometer employed in these studies was purchased with funds provided by NIH Grant 1502-RR0342 and NSF Grant BBS 86-12359. L.A.P. was a predoctoral fellow on NIH Training Grant 5 T32 GM 07313.

* To whom to address correspondence.

[⊗] Abstract published in *Advance ACS Abstracts,* April 1, 1995.

[1] Abbreviations: BPB, *p*-bromophenacyl bromide; CMC, critical micelle concentration; DODPC, deuterated dodecylphosphocholine; DQF COSY, double-quantum-filtered COSY; EM, energy minimization; HMQC, heteronuclear multiple-quantum coherence spectroscopy; NOESY, nuclear Overhauser enhancement spectroscopy; PC6, 1-(hexylthio)-2-(hexanoylamino)-1,2-dideoxy-*sn*-glycero-3-phosphocholine; PE6, 1-(hexylthio)-2-(hexanoylamino)-1,2-dideoxy-*sn*-glycero-3-phosphoethanolamine; PC9, 1-(hexylthio)-2-(nonanoylamino)-1,2-dideoxy-*sn*-glycero-3-phosphocholine; PC11, 1-(hexylthio)-2-(undecanoylamino)-1,2-dideoxy-*sn*-glycero-3-phosphocholine; PLA_2, phospholipase A_2; rMD, restrained molecular dynamics; TPPI, time-proportional phase incrementation; TOCSY, total correlation spectroscopy; TRNOE, transferred nuclear Overhauser enhancement.

0006-2960/95/0434-4943$09.00/0

1-(Hexylthio)-2-(nonanoylamino)-1,2-dideoxy-*sn*-glycero-3-phsophocholine (PC9) and 1-(hexylthio)-2-(undecanoylamino)-1,2-dideoxy-*sn*-glycero-3-phosphocholine (PC11) were synthesized via this later synthetic approach (Yu & Dennis, 1992).

Enzyme−Inhibitor NMR Sample Preparation. Cobra venom PLA_2 in 10 mM phosphate buffer at pH 6.0 was taken to dryness on a speed vac and solubilized in D_2O containing 2 mM $CaCl_2$. The inhibitors were stored in stock solutions of chloroform at −20 °C, dried under a stream of N_2, and resuspended with an aqueous solution of enzyme and $CaCl_2$. To prevent formation of vesicles and other higher order aggregates, the solution was then sonicated until it was clear. All samples were adjusted to pH 7.5 (uncorrected for deuterium isotope effect) with DCl or NaOD and contained 50 mM phosphate buffer. Protein concentrations were 0.30 mM in a sample volume of 0.45 mL. Inhibitor concentrations were 3.0 mM.

Proton-Detected 2D NMR Spectra. For the binding studies, all spectra were obtained in a Bruker AMX 500-MHz NMR spectrometer equipped with an Aspect 3000 process controller. All data were processed on a Silicon Graphics workstation using Felix 2.05 (Hare Research, Inc.). Proton spectra were collected in the phase-sensitive mode with time-proportional phase incrementation (TPPI) (Bodenhausen *et al.*, 1980) at 40 °C. The sweep width was 6250 Hz in both dimensions except for experiments modified with the Hahn echo, where the t_2 sweep width was 12 500 Hz. A continuous radio-frequency irradiation was applied during the recycle delay and during the mixing time of the NOESY (nuclear Overhauser enhancement spectroscopy) experiments to saturate the residual HOD signal. DQF (double quantum filtered) spectra (Rance *et al.*, 1983) were collected with a 1.5 s relaxation delay and processed with a sine-bell apodization in both dimensions. The TRNOE experiments were carried out with the NOESY pulse sequence (Kumar *et al.*, 1980), modified with a Hahn echo (Davis, 1989; Skelton *et al.*, 1990) to give a flat baseline and a narrow HOD resonance. The TOCSY (total correlation spectroscopy) (Bax & Davis, 1985) mixing time was 35 ms, also modified with a Hahn echo. The relaxation delay was 1.0 s. HMQC (heteronuclear multiple-quantum coherence) experiments were collected with a standard pulse sequence (Bax *et al.*, 1983; Lerner & Bax, 1986). Garp decoupling of carbon was carried out during acquisition. The ^{13}C sweep width was 7545.8 Hz and was referenced to the DSS methyl carbon at 0 ppm. The TOCSY, NOESY, and HMQC apodization used in t_2 was a Gaussian multiplier with −5-Hz line broadening and a coefficient of 0.07. A squared skewed sine-bell apodization shifted 20° was used in t_1. The first point of each block in both dimensions was multiplied by 0.5 to reduce t_1 and t_2 ridges (Otting *et al.*, 1986). The baseline was corrected wtih a third-order polynomial baseline correction routine available on Felix 2.05.

Structure Calculations. NOE data were translated into distance constraints and given an upper bound of 5 Å and a lower bound of the van der Waals radii. An additional 0.5 Å was added to distance constraints per methylene in pseudoatom constraints. Restrained molecular dynamics (rMD) and energy minimization (EM) were then employed with the Biosym Insight II program package on a Silicon Graphics workstation. All calculations were carried out *in vacuo*. Initially, the structure of the enzyme with PC6 bound, which was determined previously (Plesniak *et al.*, 1993), was altered to extend the *sn*-2 chain by three carbons. This structure was subjected to successive restrained molecular dynamics and energy minimizations. All restraint violations were penalized with a maximum force potential of 10 kcal/mol. All rMD were run by starting with high temperature (1000 K) and then gradual cooling to 300 K, for a total of 10 ps of dynamics. The structure was subsequently minimized after cooling. In the calculations, the enzyme was held constant, and the known contacts between the carbonyl and phosphate oxygens (Thunnissen *et al.*, 1990), as well as histidine 48 and the amide proton of the inhibitor (Yu & Dennis, 1991), were included in the distance constraints as described previously (Plesniak *et al.*, 1993).

In addition, several families of structures were calculated through multiple docking experiments. In these experiments PC9 was subjected to molecular dynamics in the absence of PLA_2. In these experiments, the headgroup was held fixed to facilitate docking to PLA_2 since its conformation is restrained by its coordination with the calcium and steric interactions with the protein. Furthermore, there are known crystallographic contacts between the phosphate and amide carbonyl oxygens to the calcium. Several structures with rmsd greater than 1 Å were docked to PLA_2 manually. These complexes were subjected to successive rMD and EM in the same manner described above. Five families of structures, each containing the results of 10 separate rMD calculations from five separate docking experiments, were generated for analysis.

Once the five docking experiments were completed, each conformationally distinct inhibitor was allowed to minimize in the presence of PLA_2. Because there are changes in the chemical shifts in some of the PLA_2 resonances upon binding micelles, 10 active site residues were allowed to move during calculations. However, because of computational limitations, these calculations were not done with an interface but rather with one inhibitor molecule at a time. For this reason, proposed membrane interfacial residues were still held constant.

Table 1: NOESY Spectra of Micelles

inhibitor	detergent	PLA_2	result
PE6	DODPC	−	no cross-peaks
PC6	DODPC	−	no cross-peaks
PE6	DODPC	+	no cross-peaks
PC6	DODPC	+	no cross-peaks
PC6	Triton X-100	−	spin diffusion
PC9		−	weak signal
PC9		+	cross-peaks
PC11		−	spin diffusion

RESULTS

Selection of Micellar System. Several micellar systems were examined for the possibility of using TRNOEs between micellar thioether amide inhibitors and PLA_2. Table 1 gives a brief summary of the NOESY results. Triton X-100 containing mixed micelles with the short-chain inhibitors, PE6 and PC6, gave NOESY spectra indicative of spin diffusion due to their large aggregate size. Since Triton X-100 micelles are about 90 kDa (Kushner & Hubbard, 1970), these systems cannot be used to observe TRNOEs with PLA_2 because this relaxation apparently dominates the NOESY experiments.

Micelles composed of DODPC (deuterated) presented a different problem. In the absence of PLA_2, NOESY spectra of 3.5 mM PC6 or PE6 in the presence of 60 mM DODPC did not give inhibitor cross-peaks. This is surprising since the molecular mass of DODPC micelles ranges between 21 and 27 kDa (Lauterwain *et al.*, 1979; Donne-Op den Kelder & Egmond, 1981). DODPC micelles are much smaller than Triton X-100 micelles; however, one would expect them to still be in the slow tumbling extreme on the basis of their micellar molecular mass. In addition, NOESY experiments with 60 mM DODPC, 3.5 mM PC6 or PE6, and 0.35 mM PLA_2 showed almost no evidence for the presence of either inhibitor, while the TOCSY experiments clearly confirmed their presence. Therefore, the inhibitor is still not in the slow tumbling extreme and not binding to the active site of PLA_2 with an exchange rate that would allow TRNOE measurements.

Since NOESY spectra of a sample containing 3.5 mM inhibitor and 0.35 mP PLA_2 gave TRNOEs, the addition of DODPC is causing the loss of the signal. In order to understand what happened to the exchange dynamics of the inhibitor between its free and bound forms with the addition of DODPC, a titration was carried out. The starting sample was 0.35 mM PLA_2 and 3.5 mM PC6, the typical sample conditions used to obtain TRNOEs with monomeric inhibitors (Plesniak *et al.*, 1993). As the DODPC was added to the sample, the magnitude of the NOEs steadily decreased. By 10 mM DODPC, the TRNOE signal of the inhibitor was reduced almost to the level of the noise. The CMC of DODPC is 1 mM (Hazlett & Dennis, 1985a). At 10 mM DODPC, at least 90% of it should be in micellar form. These results suggest that DODPC, which binds in the catalytic site of bovine pancreatic PLA_2 (Tomoo *et al.*, 1992), is either competing with the inhibitor or that the inhibitor is not getting incorporated into the micelle in high enough quantities.

Pure micelles of various inhibitors were used to carry out TRNOE experiments. Unfortunately, the short-chain inhibitors cannot be used for this purpose. With CMC's on the order of 10 mM, 100 mM of the short-chain inhibitor would be needed in order for 90% of the inhibitor to be in micelles. Additionally, this would require between 5 and 10 mM PLA_2 to obtain TRNOE exchange conditions (Clore & Gronenborn, 1983, 1986). The enzyme is soluble only to about 0.5 mM at pH 7.5 (L. Plesniak and E. A. Dennis, unpublished). Therefore, inhibitors with lower CMC's were necessary to observe TRNOEs in micellar systems.

Two other similar inhibitors were investigated for possible use in TRNOE experiments, PC9 and PC11. The NOESY experiments showed that the length of the *sn*-2 chain was critical to the size to the lipid aggregates formed by the inhibitors. Interestingly, a difference of two carbons in the chain length made the difference between having micelles on the border of the slow tumbling extreme and large vesicles. PC9 (see Figure 1), a thioether amide inhibitor with six carbons on the *sn*-1 chain and nine carbons on the *sn*-2 chain, aggregated into micelles that appeared to be on the border of the slow tumbling extreme. The NOESY spectra gave a few weak cross-peaks. Thus, PC9 formed pure micelles which could be used for TRNOE experiments. PC11, a thioether amide inhibitor with six carbons on the *sn*-1 chain and 11 carbons on the *sn*-2 gave NOESY spectra in the absence of enzyme dominated by spin diffusion. This inhibitor formed large aggregates even at very low concentrations, and it appeared to have too large an aggregate molecular weight to use for these studies.

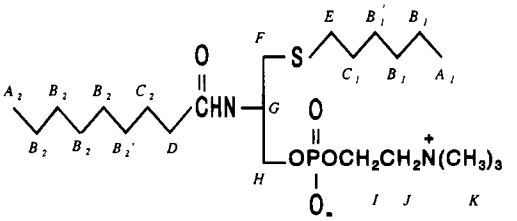

FIGURE 1: Structure of 1-(hexylthio)-2-(nonanoylamino)-1,2-dideoxy-*sn*-glycero-3-phsophocholine (PC9) with its protons labeled according to their assignments.

Chemical Shift Assignments of PC9. TOCSY, COSY, and HMQC experiments were carried out on PC9 (see Figure 2) in order to assign the protons as specifically as possible (see Table 2). The seven methylene groups on the *sn*-2 chain of PC9 give rise to many degenerate proton signals. As previously observed with shorter chain inhibitors (Plesniak *et al.*, 1993), the methylene protons α to the amide on the *sn*-2 chain, D, are shifted upfield from the methylene protons α to the thioether on the *sn*-1 chain, E. This dispersion aids in interpretation of NOESY spectra. An interesting observation in the assignments is the magnetic nonequivalence of the methylene protons β to the amide, $C2_a$ and $C2_b$, which was not observed with the shorter chain inhibitors. These protons give separate signals in samples both with and without the enzyme present; however, in the absence of enzyme, there is evidence of exchange broadening between the two states which resolves into two signals in the TRNOE studies. The assignment of the two resonances belonging to the $C2_a$ and $C2_b$ protons was determined by COSY experiments (data not shown) and verified by the HMQC experiment (Figure 2) where these two protons were shown to be attached to the same carbon.

The proton signals of the γ-methylenes (B1′ and B2′), one carbon down on either chain, are shifted slightly downfield from the rest of the methylenes in the chain. This assignment was also confirmed by the HMQC experiment, where there is only one carbon chemical shift at the corresponding proton chemical shifts. In the *sn*-1 chain, this leaves two remaining degenerate methylene groups. However, in the *sn*-2 chain, there are four degenerate methylene groups. The HMQC experiment shows slight shifts between some of these four methylenes; however, with exchange-broadened line widths, even 2-D experiments cannot resolve these signals. Attempts have been made to use the carbon chemical shifts to distinguish between the methylenes in the TRNOE experiments, utilizing natural abundance 2D HMQC-NOESY experiments. The experiment worked for the stronger, resolved NOE resonances. Table 2 gives the chemical shifts of the proton and their assignments for PC9.

TRNOEs with Pure Micelles. NOESY experiments were carried out on the pure micelles of PC9 in the presence of PLA_2. Because the CMC of PC9 is 0.3 mM (Yu & Dennis, 1992), at 3 mM, at least 90% of the inhibitor should be partitioned into the micellar form. Experiments were carried out on a sample containing 3 mM PC9 and 0.3 mM PLA_2. These conditions resulted in the proper exchange rates for TRNOEs for intramolecular inhibitor NOESY cross-peaks (see Figure 3). There were many cross-peaks present in these experiments that were not observed in the NOESY spectrum of the pure micelle without PLA_2, and all the cross-peaks

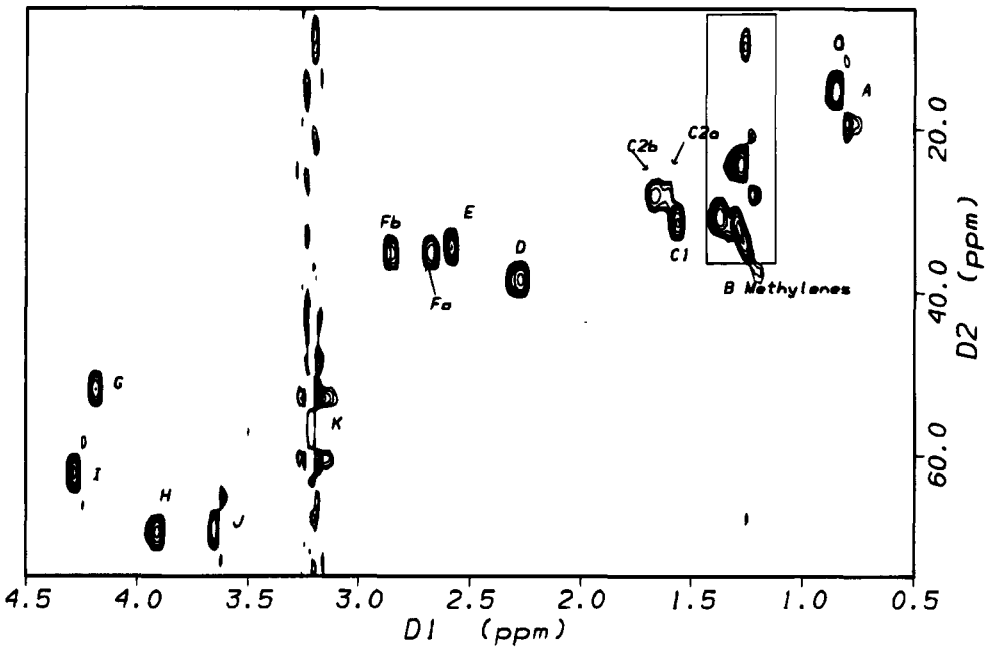

FIGURE 2: HMQC spectrum of PC9 to facilitate the assignment of the methylene protons on the nine-carbon *sn*-2 chain. The protons β to the amide are magnetically nonequivalent, giving rise to the two proton signals $C2_a$ and $C2_b$.

Table 2: Chemical Shifts of PC9 (ppm)

proton	PC9	+PLA_2	+BPB−PLA_2
A1	0.85	0.82	0.78
A2	0.85	0.80	0.79
B1	1.28	1.18	1.16
B2	1.31	1.23	1.16
B2′	1.37	1.28	1.22
C1	1.56	1.47	1.42
$C2_a$	1.58	1.54	1.46
$C2_b$	1.67	1.62	1.54
D	2.27	2.21	2.14
E	2.58	2.49	2.43
F_a	2.67	2.63	2.60
F_b	2.86	2.82	2.76
G	4.19	4.18	4.16
H	3.90	3.90	3.90
I	4.28	4.26	4.21
J	3.66	3.56	3.50
K	3.21	3.09	3.09

were of greater intensity. In addition, there were new cross-peaks between the glycerol backbone and the two acyl chains, which were not observed in the NOESY experiments with the short-chain inhibitors, PC6 and PE6 (Plesniak *et al.*, 1993). NOESY experiments were carried out with mixing times of 75, 100, and 125 ms to confirm that cross relaxation was not the result of spin diffusion. NOEs were assigned distances ranging between the van der Waals radii and 5 Å.

BPB-Modified PLA_2 TRNOEs. The same NOESY experiment was carried out with BPB-modified PLA_2 as shown in Figure 4C. The BPB modification prevents specific binding to the active site of PLA_2 with monomeric substrate analogue inhibitors (Plesniak *et al.*, 1993). In the present case, a similar inhibitor was used; however, due to the longer *sn*-2 chain, the inhibitor is now present in micellar form. The presence of NOEs in the experiments with PC9 indicated that the enzyme was bound to the micelles or that there was residual binding in the active site of PLA_2. However, the NOESY spectrum (Figure 4C) contained a few different cross-peaks than the spectrum (Figure 4B) with the unmodified PLA_2. This indicated an additional mode of binding,

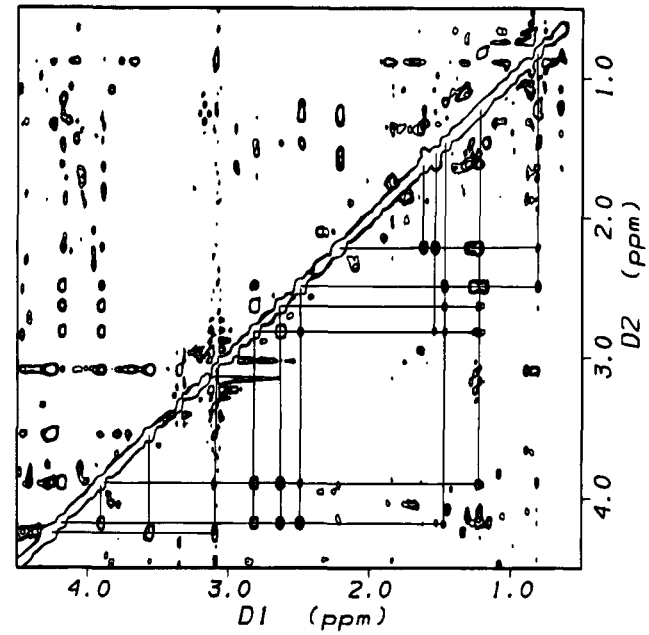

FIGURE 3: Section of a typical 125-ms mixing time NOESY spectrum of 3 mM PC9 and 0.3 mM PLA_2 which yields TRNOEs of the inhibitor. The intramolecular TRNOEs are marked with lines. The remaining peaks are PLA_2 peaks.

possibly interfacial binding. In addition, the TRNOE experiment with unmodified enzyme had several cross-peaks which indicated the proximity of the two acyl chains. There was also evidence of chain proximity in the experiments with the BPB-inhibited enzyme, although not as extensive. At least three of the NOEs indicating an interaction between the two chains were missing: C_{2b} E, C_{2a} F_b, and B_1 F_b.

Structure Calculations. Structure calculations for PC9 were undertaken using the distance constraints obtained from the NOESY experiments. The information from the NOESY experiments was interpreted with caution for two main reasons. First, there was a high degree of degeneracy of the methylene protons on the two chains. This made assignment of the NOE cross-peaks uncertain. There were

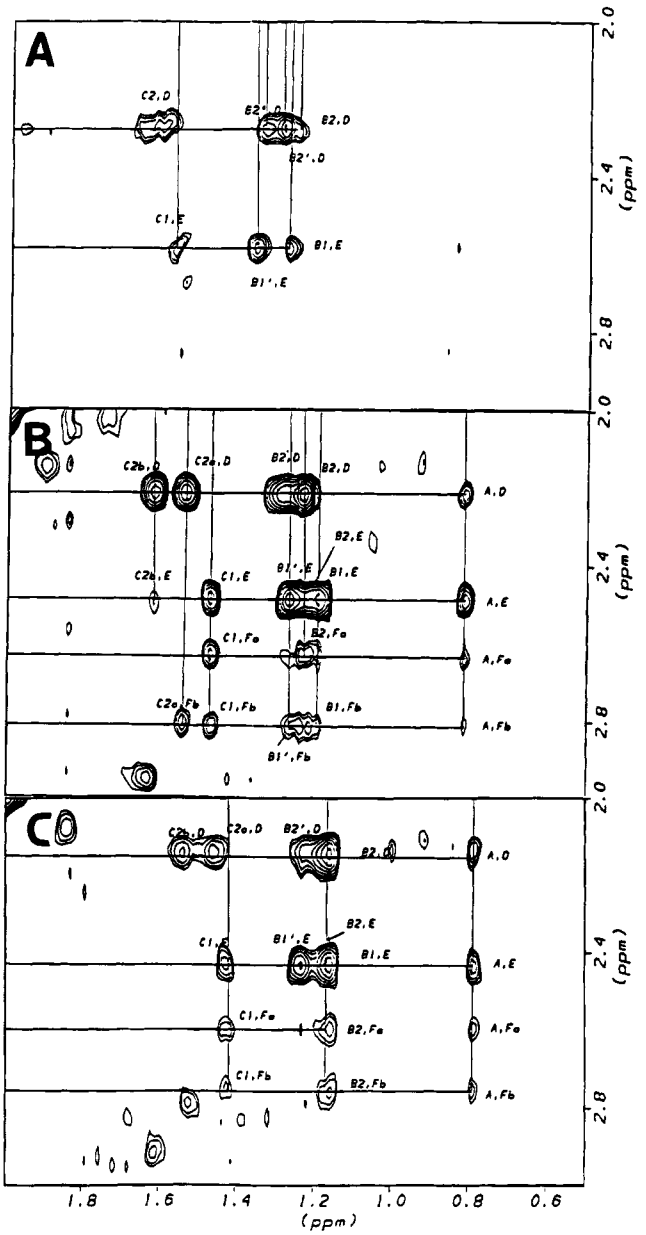

FIGURE 4: Sections of NOESY spectra around the methylene cross-peaks to D and E. The NOESY spectrum was obtained with a 125-ms mixing time of (A) 3.0 mM PC9, (B) 3.0 mM PC9 with 0.3 mM PLA_2 added to the inhibitor, and (C) 3 mM PC9 and 0.3 mM BPB-modified PLA_2.

several differences between the BPB-PLA_2 NOESY spectra and the PLA_2 NOESY spectra and much greater intensity in the signal in the unmodified PLA_2 relative to the diagonal. However, there were a couple of cases where the cross-peak intensity did not increase with the BPB-PLA_2 NOESY spectra (A_2 F_a, A_2 F_b). For this reason, these cross-peaks were not included in the structure calculations since it was not certain whether these cross-peaks were a result of interfacial binding or active site binding. Because of these complications, the NOEs were not classified by their intensity into strong, medium, and weak; rather, they were used to constrain protons within 5 Å of each other. There were a total of 32 NOE constraints and 3 constraints derives from crystallographic data (see Table 3). These constraints were employed as described in the Materials and Methods section.

Several families of structures were generated through a variety of calculation approaches. Figure 5 shows five

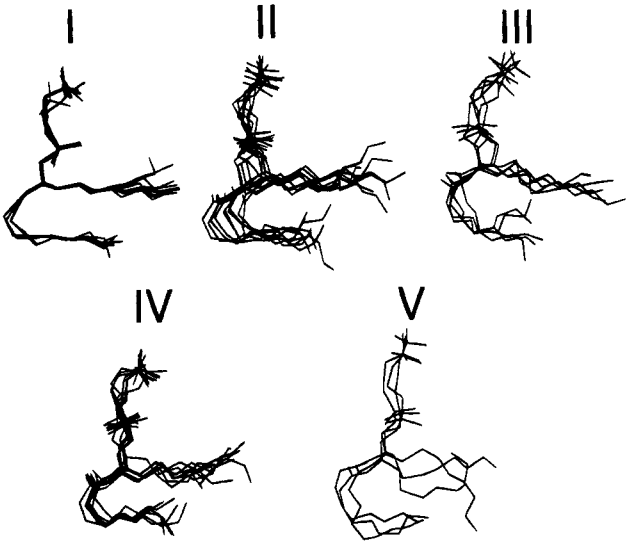

FIGURE 5: Five families of structures generated for PC9.

Table 3: NOE Restraints

proton pair	max distance (Å)
J I	5.0
k I	5.0
k J	5.0
F_b E	5.0
F_b A_2	5.0
F_b H	5.0
F_b G	5.0
F_a G	5.0
F_a H	5.0
E H	5.0
E G	5.0
C_2' H	5.0
C_2' D	5.0
C_2' G	5.0
C_2' E	5.0
C_2' F_b	5.0
C_1 E	5.0
C_1 G	5.0
C_1 F_a	5.0
C_1 F_b	5.0
C_2 D	5.0
B_1' F_a	5.0
B_1' E	5.0
B_2 F_b	6.0
B_2 D	6.5
B_2 F_a	6.0
B_2 H	6.5
B_1 E	5.5
B_1' F_b	5.0
E A_2	5.0

families of structures. Of the 35 constraints employed in the calculations, there were generally between two and five NOE violations. Family I is the result of extending the *sn*-2 chain on the bound structure of PC6, the short-chain inhibitor, and proceeding with repeated rMD and EM calculations. Families II, III, and IV are the results of docking PC9 from five different starting conformations and repeating successive rMD and EM. Of these three families, family IV has the lowest average energy by about 10 kcal and generally had fewer NOE violations. Family V is similar to family I in that its origin is with the bound structure of PC6, the short-chain inhibitor. Family V is the result of taking the bound PC6 *sn*-2, extending it by three carbons, and running repeated rMD and EM calculations; however, this time nine active site residues, Leu-2, Phe-5, Trp-19, Trp-20, Asp-21, Phe-

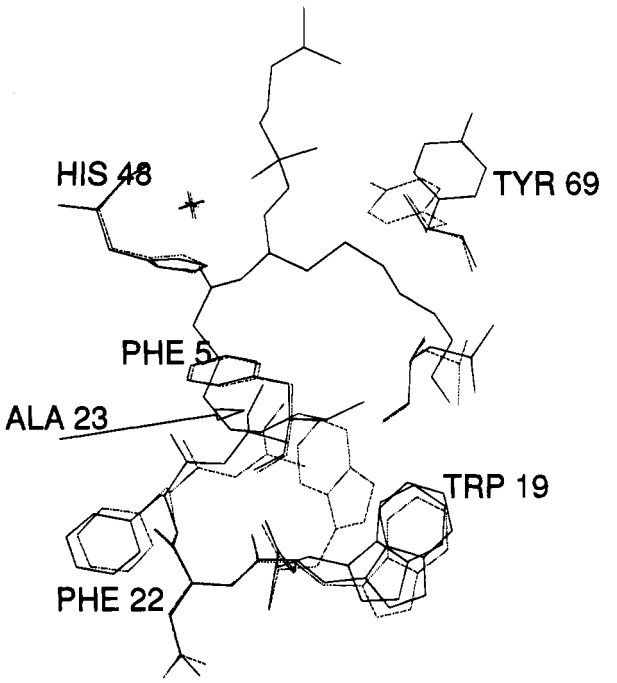

FIGURE 6: Results of the family V structure calculations on PC9 shown in the active site of PLA_2. The solid lines indicate the original positions of the side chains of PLA_2. The stippled lines show the final positions of the residues.

22, Ala-23, His-48, and Tyr-69, were allowed to move. Previously, it had been suggested that Tyr-69 is the only residue in the active site of the porcine pancreatic PLA_2 to occupy two separate states upon inhibitor binding (Lauterwain *et al.*, 1979). Family V gave the lowest energy structures and had few NOE violations. In the calculations, the side chains that consistently showed the most movement were Trp-19, Ala-23, and Tyr-69. Trp-20 changed its orientation in about half of the calculations (see Figure 6). All the other residues maintained their original orientations found in the crystal structure.

Structure of PLA_2-Bound PC9. The result of 10 separate cycles of rMD and EM structure calculations is shown in Figure 5. Figure 7A shows family I from this figure with the hydrophobic residues in the substrate binding pocket. According to previous studies, maximal binding affinity occurs with nine carbons in the *sn*-2 chain (Yu & Dennis, 1992). At this length, there are as many as five residues close enough to contribute hydrophobic contacts for binding. These residues are Phe-5, Trp-19, Leu-2, Ala-23, barely reaching the end of hydrophobic contacts with Leu-2, and Phe-106. Close by, but not quite in range, is Phe-22.

Comparatively, the *sn*-1 chain has much less interaction with the enzyme. This is in agreement with studies that have shown that the length of the *sn*-1 chain is not part of the minimum substrate requirement for the porcine pancreatic enzyme (Van Deenen & DeHaas, 1963). The *sn*-1 chain has a lot of surface accessibility in contrast to the buried *sn*-2 chain. The *sn*-2 chain has just barely reached the end of hydrophobic contacts with Leu-2 and Trp-19.

DISCUSSION

Transferred NOEs. Obtaining and interpreting transferred NOEs between a lipid aggregate and an enzyme are particularly challenging. Reports of NMR studies are limited to proteins bound to micellar interfaces (Peters *et al.*, 1992; Brown & Wuthrich, 1981; Brown *et al.*, 1982) where the protein or peptide is observed. Such studies have focused on the structure of the macromolecule when bound to an interface. Our goal has been to determine the structure of the inhibitor, a phospholipid analogue in a micellar interface when bound to PLA_2. For such studies, two conditions must be met. First, exchange conditions for TRNOEs must be met. This involves controlling protein:inhibitor ratios as well as maintaining micelle conditions. Second, the state of the lipid aggregate must be controlled and characterized. Vesicles have too large a molecular weight, causing spin diffusion to dominate the NOESY spectra. Although smaller than vesicles, micelles can also have large aggregate mass; however, fluidity within the aggregate may lower the effective correlation time to bring the lipid out of the slow tumbling extreme. The first goal was to find a low molecular weight micelle where spin diffusion would not be a problem in the NOE experiments. The size of pure micelles of the thioether amide inhibitors has not been determined. However, the phospholipid micelles formed by dihexanoyl-PC have been determined to have a micellar molecular mass between 15 000 and 20 000 Da (Tausk *et al.*, 1974). The micellar mass of diheptanoyl-PC can range between 20 000 and 100 000 Da (Tausk *et al.*, 1974). These phospholipids differ from the inhibitors only by the replacement of the *sn*-1 and *sn*-2 esters with a thioether and an amide, respectively. Consequently, the micellar molecular mass of the dihexanoyl-PC may approximate the micellar molecular mass of PC. The micelles should be significantly smaller than mixed micelles with Triton X-100 of 80 000−100 000 Da molecular mass (Robson & Dennis, 1977) or egg PC vesicles which have a molecular mass of 2×10^6 Da (Huang & Lee, 1973).

In the ideal case, the NOESY spectra of micelles in the absence of PLA_2 would show no cross-peaks but still would show strong NOESY cross-peaks in the presence of PLA_2. In this case, the observed NOEs of the enzyme−inhibitor complex would not reflect the lipid aggregate structure but rather would be indicative of enzyme−inhibitor interactions.

Studies with DODPC and Triton X-100. Our first attempts at observing TRNOEs with micellar inhibitors were with DODPC; however, the short-chain inhibitor did not appear to comicellize with DODPC micelles in high enough quantities to use for TRNOE experiments. In these NOESY experiments, the inhibitor was not in the slow tumbling extreme. Since the DODPC micelles are in the 21−27 kDa molecular mass range (Leuterwain *et al.*, 1979; Donne-Op den Kelder & Egmond, 1981), a size which should be in the slow tumbling domain, it is likely that the inhibitor was not fully incorporated into micelles. In an effort to micellize the short-chain inhibitors, experiments with Triton X-100 micelles were carried out. However, spin diffusion dominated the NOESY spectra, and no differences were observed with PLA_2 was added. Experiments with these micelles were not a sensitive measure of lipid binding to PLA_2, nor a system to determine bound lipid conformation. These results are in agreement with those of other investigators who have attempted to observe the high-resolution NMR signal of bacteriorhodopsin in Triton X-100 micelles (Seigneuret & Neumann, 1991).

Studies with Pure Micelles. Preliminary NOESY studies with longer chain hexylthio amide inhibitors as micelles were carried out to find a micelle of the right size for these experiments. The effect of the *sn*-2 chain length on the CMC

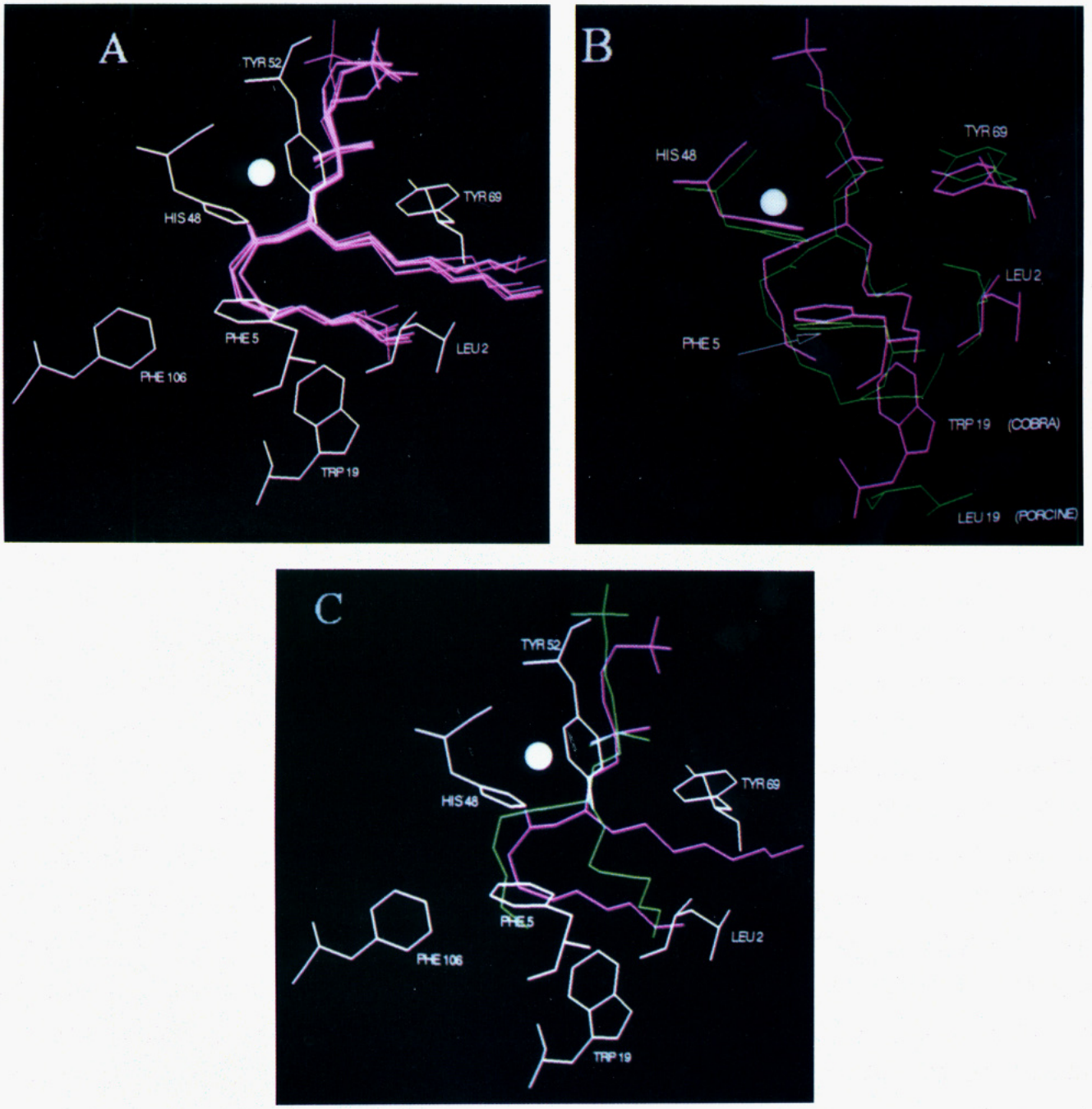

FIGURE 7: (A) Result of 10 successive rMD and EM calculations. Several starting conformations were generated in the absence of the enzyme. This is the result of docking one such structure and then repeatedly subjecting it to dynamics and minimization. The inhibitor is shown in pink, and the side chains of PLA_2 are shown in white. (B) Overlay of the porcine PLA_2 crystal structure complex (green lines) with the alkyl amide inhibitor and the cobra PLA_2 structure (pink lines) with PE6. The short-chain inhibitor's structure was previously determined (Plesniak *et al.*, 1993). The longer *sn*-2 chain in the porcine pancreatic active site would penetrate the plane of Trp-19 in the cobra venom PLA_2's hydrophobic pocket. (C) Overlay of PC6 (green lines) and PC9 (pink lines) in the cobra venom PLA_2 active site. The extension of the *sn*-2 chain forces the inhibitor to adopt a different conformation.

of these inhibitors has already been documented (Yu & Dennis, 1992); however, the size of these micelles was not known. The high CMC, 10 mM, of the short-chain inhibitors, PE6 and PC6, prohibits their use in micelle form for TRNOE studies. The NOESY spectrum of PC9 at 125 ms showed very weak negative cross-peaks between protons that were connected through bonds. From these experiments we determined that these micelles were on the border between between the slow tumbling and the fast tumbling extremes. The inhibitor with the best combination of CMC and micelle size was PC9. With a CMC of 0.3 mM, PC9 is in the perfect range for TRNOE studies with a 10−20-fold excess of ligand. Additionally, it is advantageous to limit the length of the *sn*-2 chain to avoid degenerate proton methylene signals in NMR experiments.

NMR Spectra of the PC9−PLA_2 Complex. TRNOE studies of the complex of PLA_2 and PC9 gave good NOESY spectra with inhibitor intramolecular NOEs of high intensity relative to the protein's NOEs (see Figure 3 and Figure 4B). At 3 mM PC9 and 0.3 mM PLA_2, the enzyme is soluble, the lipid is observable by proton NMR, and TRNOE exchange conditions were met. There were several intramolecular NOEs in the TRNOE experiments which were not present in the short-chain inhibitor NOESY spectra. Because

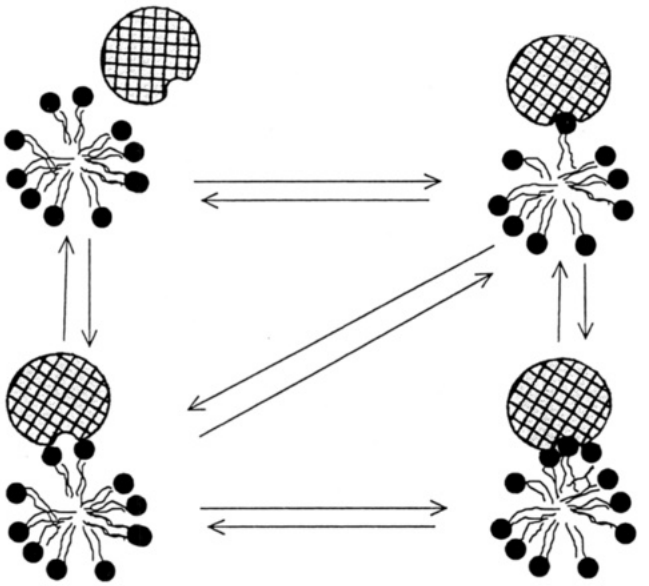

FIGURE 8: Variety of bound and free forms of PLA_2 in equilibrium with PC9 phospholipid in micelles.

the methylene protons that are β to the amide are nonequivalent, more detailed distance constraints were obtained. In addition, there was a new NOE between the *sn*-2 and *sn*-1 chains, as well as many new NOEs to the glycerol backbone not observed in the previous studies (see Figure 4B). The new NOE and the β-methylene protons indicate that there is a different conformation of the chains in the active site. Unfortunately, there was also a much greater degree of degeneracy among the methylenes with PC9, and the interpretation of NOE cross-peaks among the methylenes was not certain.

One other problem with the PC9 NOESY experiments is that the intermolecular NOEs with PLA_2 were uninterpretable. At these concentrations, the cobra enzyme was in exchange between soluble and micelle-bound forms and undergoes some averaging of the chemical shift changes. See Figure 8 for the variety of free and bound forms possible. At 3 mM lipid, the micelle concentration should be much less than 0.3 mM, the concentration of the enzyme. It is likely that some enzyme was free even if more than one enzyme can bind per micelle. Previous studies with porcine PLA_2 showed changes in the chemical shifts of aromatic residues upon binding to micelles and an averaging of signals until all the enzyme was bound (Peters *et al.*, 1992). In the region of the NOESY spectra between the methylene region of the inhibitor and the aromatic side chains of PLA_2, there are exchange-broadened NOEs. These NOEs are narrow peaks in the inhibitor chemical shifts but are broad in the PLA_2 shift, indicating that PLA_2 is in intermediate exchange in the chemical shift time scale.

BPB−PLA_2 NOESY Spectra. The same NOESY experiments were carried out with PLA_2 modified by BPB. In the previous studies with BPB−PLA_2 with monomeric inhibitors, there was little or no specific binding to the active site. In contrast, the BPB−PLA_2 bound quite effectively to the micelles of PC9 as evidenced by the intensity of the NOEs (see Figure 4C). There were differences between the BPB−PLA_2 and PLA_2 experiments. In addition, the cross-peaks of the BPB−PLA_2 experiment gave lower intensities, about 10% of the volume of the cross-peaks observed with the unmodified enzyme. However, the presence of NOEs indicated that binding definitely occurs with the modified enzyme. Some of the NOEs that were unique to the long-chain PC9 when bound to the unmodified PLA_2 were missing; however, there was still evidence that the two chains interact. There were also some intermolecular NOEs between the BPB−PLA_2 and PC9. These were uninterpretable as described for the unmodified enzyme.

Importance of sn-1 Chain Length. Our studies did not find significant interactions between the *sn*-1 chain of the inhibitor and the enzyme. A recent paper (de Haas *et al.*, 1993) speculated as to why the *sn*-1 chain of alkyl amide inhibitors with six carbons had the highest inhibitory potency when the crystal structures of inhibitor−PLA_2 complexes showed clearly that there were no major hydrophobic contacts between the *sn*-1 chain and the enzyme.

Comparison of the Bound Structure of PE6 and PC9. If the crystal structure of the porcine pancreatic phospholipase A_2 (Thunnissen *et al.*, 1990) with an inhibitor bound is compared to the crystal structure of the cobra PLA_2 (Fremont *et al.*, 1993), it is not surprising that the TRNOE NOESY spectra of PC9 show different cross-peaks from the glycerol backbone to the two chains than PE6. The inhibitor in the porcine pancreatic PLA_2 is a phosphoglycol analogue with an amide in place of the *sn*-2 ester and a four-carbon alkyl chain extending from the *sn*-2 backbone carbon. The inhibitor in cobra PLA_2 differs by having an *sn*-1 chain with a thioether. These two inhibitors have similar bound conformations; however, this cannot be the case for a longer chain inhibitor in the cobra PLA_2 active site.

Figure 7B shows the overlay of the porcine active site residues determined by crystallography with a similar structure of the cobra PLA_2 with the short-chain inhibitor docked as determined by crystallography and NMR (Plesniak *et al.*, 1993). If the longer *sn*-2 chain of the porcine inhibitor is traced through the cobra active site, the *sn*-2 chain would penetrate the plane of the Trp-19 of the cobra enzyme. This is not possible in the binding of a long-chain inhibitor in the cobra PLA_2 active site. Consequently, there must be either a shift in the glycerol backbone or a sharp curve of the *sn*-2 chain around Trp-19. Figure 7C shows the structure of cobra PLA_2 with the short-chain inhibitor compared to the structure of cobra PLA_2 with PC9, a long-chain inhibitor, as determined by TRNOEs. There is a shift of the entire inhibitor's positioning in the active site. Both structures are consistent with their NOE constraints. In addition, if the *sn*-2 chain of the short-chain inhibitor is lengthened by three carbons in the active site, and then subjected to rMD and EM, the same shift is observed in the long-chain inhibitor's orientation. These calculations are done with all the residues of PLA_2 held fixed. Calculations carried out this way allow for a larger statistical sampling of inhibitor conformations but may not find the lowest energy minimum for the bound inhibitor if there is a conformational change in PLA_2 upon inhibitor binding.

The calculations that were carried out to allow the active site residues to move consistently show that Trp-19 reorients its indole ring to allow for favorable interaction with the *sn*-2 chain and to allow the chain to settle into the hydrophobic pocket of the enzyme. We believe the reorientation of Trp-19 to be significant in the active site binding of the inhibitor because this complex has the lowest energy and meets all NOE constraints. Additionally, Ala-23 also

orients itself to more favorably interact with the *sn*-2 chain, moving closer to the B2 methylene protons.

Summary. These experiments demonstrate that it is feasible to observe TRNOEs between an inhibitor aggregated in a micelle and a macromolecule as long as the micelles of the inhibitor meet several criteria. The CMC and size of the micelles for the PC9 inhibitor are optimal for use in TRNOE studies. The NOESY data should be interpreted with caution since contributions can be made by interfacial binding and active site binding of the lipid. Covalent modification of the enzyme has been employed to distinguish between these two modes of binding. The inhibitor, although very similar to a previously studied short-chain inhibitor, has a very different conformation in the active site. This is due primarily to steric interactions between the *sn*-2 chain hydrophobic residues which extend into the hydrophobic pocket. Finally, the structures agree with kinetic studies that have suggested that the length of the hydrophobic contacts with the *sn*-2 chain extends at least to the ninth carbon.

ACKNOWLEDGMENT

We thank Professor Elizabeth A. Komives for critical reading of the manuscript and Scott C. Boegeman for valuable discussions in carrying out the experiments.

REFERENCES

Bax, A., & Davis, D. G. (1985) *J. Am. Chem. Soc. 107*, 2820.
Bax, A., Griffey, R. H., & Hawkins, B. L. (1983) *J. Magn. Reson. 55*, 301.
Bhatia, S. K., & Hajdu, J. (1988) *Tetrahedron Lett. 29*, 31−34.
Bodenhausen, G., Vold, R. L., & Vold, R. R. (1980) *J. Magn. Reson. 37*, 93−106.
Brown, L. R., & Wuthrich, K. (1981) *Biochim. Biophys. Acta 647*, 95−111.
Brown, L. R., Braun, W., Kumar, A., & Wuthrich, K. (1982) *Biophys. J. 37*, 319−328.
Clore, M. G., & Gronenborn, A. M. (1983) *J. Magn. Reson. 53*, 423−442.
Clore, M. G., & Gronenborn, A. M. (1986) *J. Mol. Biol. 190*, 259−267.
Davidson, F. F., Hajdu, J., & Dennis, E. A. (1986) *Biochem. Biophys. Res. Commun. 137*, 587−592.
Davis, D. G. (1989) *J. Magn. Reson. 81*, 603−607.
de Haas, G. H., Dijkman, R., Lugtigheid, R. B., Dekker, N., Van den, Berg, L., Egmond, M. R., & Verheij, H. M. (1993) *Biochim. Biophys. Acta 1167*, 281−288.
Dekker, N., Peters, A. R., Slotboom, A. J., Boelens, R., Kaptein, R., Dijkman, R., & de Haas, G. (1991) *Eur. J. Biochem. 193*, 601−607.
Dennis, E. A. (1983) in *The Enzymes* (Boyer, P., Ed.) 3rd ed., Vol. 16, pp 307−353, Academic Press, New York.
Dennis, E. A. (1994) *J. Biol. Chem. 269*, 13057−13060.
Donne-Op den Kelder, G. H., & Egmond, M. R. (1981) *Biochemistry 20*, 4047−4078.
Fremont, D. H., Anderson, D., Wilson, I. A., Dennis, E. A., & Xuong, N.-H. (1993) *Proc. Natl. Acad. Sci. U.S.A. 90*, 342−346.
Hazlett, T. L., & Dennis, E. A. (1985a) *Biochemistry 24*, 6152−6158.
Hazlett, T. L., & Dennis, E. A. (1985b) *Toxicon 23*, 457−466.
Hazlett, T. L., Deems, R. A., & Dennis, E. A. (1990) *Adv. Exp. Med. Biol. 279*, 49−64.
Huang, C.-H., & Lee, L.-P. (1973) *J. Am. Chem. Soc. 95*, 234−239.
Kumar, A., Ernst, R. R., & Wuthrich, K. (1980) *Biochem. Biophys. Res. Commun. 95*, 1−6.
Kushner, L. M., & Hubbard, W. D. (1970) *Am. J. Med. 49*, 590−608.
Lauterwain, J., Boesch, C., Brown, L. R., & Wuthrich, K. (1979) *Biochim. Biophys. Acta 556*, 244−624.
Lerner, A., & Bax, A. (1986) *J. Magn. Reson. 69*, 375−380.
Otting, G., Widmer, G., & Wuthrich, K. (1986) *J. Magn. Reson. 66*, 187−193.
Peters, A. P., Dekker, N., van den Berg, L., Boelens, R., Kaptein, R., Slotboom, A. J., & de Haas, G. H. (1992) *Biochemistry 31*, 10024−10030.
Plesniak, L. A., Boegeman, S. C., Segelke, B. W., & Dennis, E. A. (1993) *Biochemistry 32*, 5009−5016.
Rance, M., Sorensen, O. W., Bodenhausen, G., Wagner, G., Ernst, R. R., & Wuthich, K. (1983) *Biochem. Biophys. Res. Commun. 117*, 479−485.
Reynolds, L. J., & Dennis, E. A. (1991) in *Methods in Enzymology* (Dennis, E. A., Ed.) Vol. 197, pp 359−365, Academic Press, Orlando, FL.
Roberts, M. F., Demms, R. A., Mincey, T. C., & Dennis, E. A. (1977) *J. Biol. Chem. 252*, 2405−2411.
Robson, R. J., & Dennis, E. A. (1977) *J. Phys. Chem. 81*, 1075−1078.
Seigneuret, M., & Neumann, J.-L. (1991) *J. Biol. Chem. 266*, 10066−10069.
Skelton, N. J., Forsen, S., & Chazin, W. J. (1990) *Biochemistry 29*, 5752−5761.
Tausk, R. J. M., Van Esch, J., Karmiggelt, J., Voordouw, G., & Overbeek, J. Th. G. (1974) *Biophys. Chem. 1*, 184−203.
Thunnissen, M. M., Ab, E., Kalk, K. H., Drenth, J., Dikstra, B. W., Kuipers, O. P., & Dijkman, R. (1990) *Nature 347*, 689−691.
Tomoo, K., Ohishi, H., Doi, M., Ishida, T., Ikeda, K., & Mizuno, H. (1992) *Biochem. Biophys. Res. Commun. 187*, 821−827.
Van Deenen, L. L. M., & DeHaas, G. H. (1963) *Biochim. Biophys. Acta 70*, 469−471.
Yu, L., & Dennis, E. A. (1991) *Proc. Natl. Acad. Sci. U.S.A. 88*, 9325−9329.
Yu, L., & Dennis, E. A. (1992) *J. Am. Chem. Soc. 114*, 8757−8763.
Yu, L., Deems, R. A., Hajdu, J., & Dennis, E. A. (1990) *J. Biol. Chem. 265*, 2657−2664.

BI942307E